Ellipticine Binds to a Human Telomere Sequence: An Additional Mode of Action as a Putative Anticancer Agent?

Saptaparni Ghosh,[†] Anirban Kar,[‡] Shantanu Chowdhury,[‡] and Dipak Dasgupta*,[†]

[†]Biophysics Division, Saha Institute of Nuclear Physics, Block-AF, Sector- I, Bidhan Nagar, Kolkata 700064, India
[‡]Proteomics and Structural Biology Unit, Institute of Genomics and Integrative Biology, CSIR, Room 307, Mall Road, Delhi 110007, India

S *Supporting Information*

ABSTRACT: Polyguanine sequences fold into G-quadruplex structures in the presence of monovalent cations. It is accepted that the telomeric DNA region consists of G-quadruplex structure. There are reports that potential G-quadruplex forming motifs are also present in the promoter region of some proto-oncogenes such as c-myc, c-kit, KRAS, etc. Small molecules with the potential to stabilize the telomeric DNA quadruplex have emerged as potential anticancer agents. We have studied the interaction of ellipticine, a putative anticancer agent from a plant source, with a human telomeric DNA sequence (H24). Spectroscopic and calorimetric studies indicate that the association of ellipticine with H24 is an entropically driven phenomenon with a 2:3 (H24:ellipticine) stoichiometry. Though ellipticine binding does not induce any major structural perturbation in H24, the association leads to formation of a complex with enhanced thermal stability. An assay with the telomerase repeat amplification protocol shows that ellipticine inhibits telomerase activity in MDAMB-231 breast cancer cell line extracts. This is the first report of the quadruplex binding ability of ellipticine. Using the results, we propose that along with DNA intercalation and/or topoisomerase II inhibition, interaction with the telomeric DNA region and the resultant inhibition of telomerase activity might be an additional mode of action for its anticancer property.
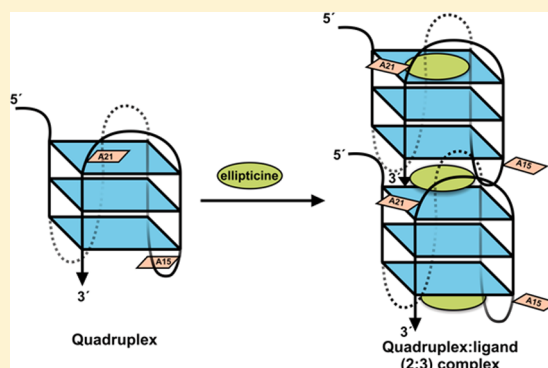
The ends of the eukaryotic chromosomes have a special nucleoprotein structure known as telomere.[1] Telomeres play an important role in cellular aging and cancer.[2] In humans, the telomere consists of tandem repeats of d(TTAGGG) 5–8 kb in length in a double-helical form. They end in a single-stranded 3′ overhang of approximately 100–200 bases in length. Their replication is dependent on the enzyme telomerase. Telomerase expression is tightly controlled in normal somatic cells in which the telomere becomes shorter after each round of cell division. Telomerase is overexpressed in cancer cells in which the telomere does not become shorter. It has been found that formation of stable G-quadruplex structures in the single-stranded telomeric region inhibits telomerase activity. The telomeric G-quadruplex has thus emerged as a potential target for anticancer agent(s). They bind to the telomeric quadruplex, thereby stabilizing it and inhibiting telomerase activity.

Ellipticine (5,11-dimethyl-6*H*-pyrido[4,3*b*]carbazole) (Figure 1), a plant alkaloid from *Apocyanaceae* plants, has high efficiency against several types of cancer with limited toxic side effects.[3] Available reports ascribe its antineoplastic activity to DNA intercalation[4] and/or inhibition of topoisomerase II.[3,5,6] Here we have investigated the mechanism of interaction of the putative anticancer agent ellipticine with a human telomeric DNA sequence (H24, 5′-TTAGGGTTAGGGTTAGGGTTA-
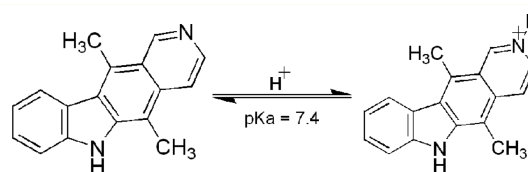

Figure 1. Structure of ellipticine. The protonated form intercalates into double-stranded DNA.

GGG-3′) using spectroscopic and calorimetric techniques. In addition, we have conducted a TRAP (telomeric repeat amplification protocol) assay to demonstrate the potential telomerase inhibitory activity of the agent using MDAMB-231 breast cancer cell line extracts. From the results of this study, we propose that human telomeric DNA, which folds into a quadruplex structure, is an additional and/or alternate target leading to the antineoplastic activity of ellipticine.

■ EXPERIMENTAL PROCEDURES

Materials. Ellipticine, monobasic potassium phosphate, dibasic potassium phosphate, and the desalted and high-

performance liquid chromatography-purified human telomeric DNA sequence (H24) were purchased from Sigma Chemical Corp. Dimethyl sulfoxide (DMSO) was purchased from Fisher Scientific. All buffers were prepared in Milli-Q water from a Millipore Water System and filtered through 0.1 μm filters from Millipore prior to use. All experiments were performed in 10 mM potassium phosphate buffer (pH 6.8) containing 150 mM KCl unless otherwise mentioned.

Ellipticine was dissolved in freshly distilled DMSO and stored at 4 °C. The concentration of the stock drug solution was determined from the absorbance using an ε_{295} of 60000 M^{-1} cm^{-1}.[7] In all the experiments, the DMSO content was kept below 0.5% (v/v).

H24 was dissolved in 10 mM potassium phosphate buffer (pH 6.8) containing 150 mM KCl, heated to 90 °C in a water bath, and held for 10 min. The sample was allowed to equilibrate to room temperature slowly and stored at 4 °C for 48 h. It was then dialyzed against the same buffer for 24 h. The concentration of H24 was determined by the absorbance using an ε_{260} of 244600 M^{-1} cm^{-1}. The molar extinction coefficient of H24 was determined using the nearest neighbor approximation model. Characteristic CD spectra of H24 confirmed the formation of (3+1) hybrid structure.[8] Unless stated otherwise, the concentration of H24 is expressed in terms of the oligomer.

Methods. *Fluorescence Spectroscopy.* Fluorescence spectra were recorded on an LS 55 luminescence spectrometer (Perkin-Elmer) fitted with a water circulation system to maintain a constant temperature. To determine the dissociation constant of the quadruplex–ligand interaction, we titrated 5 μM ellipticine with an increasing concentration of H24 until there was no further change in the emission intensity with an increase in the input oligomer concentration. Emission spectra corresponding to excitation at 320 nm were recorded 5 min after each addition to ensure equilibration of the temperature and complete complex formation. The binding isotherm was obtained from a plot of $\Delta F/\Delta F_{max}$ (at 520 nm) as a function of input H24 concentration. The experimental points for the binding isotherm were fit using the equation[9]

$$C_0(\Delta F/\Delta F_{max})^2 - (C_0 + C_p + K_d)(\Delta F/\Delta F_{max}) + C_p = 0 \tag{1}$$

where C_0 is the initial ellipticine concentration, ΔF is the change in fluorescence at 520 nm after addition of each aliquot of H24, ΔF_{max} is the same parameter when ellipticine is totally bound to H24, and C_p is the concentration of H24 added. ΔF_{max} was estimated from the double-reciprocal plot of $1/\Delta F$ versus $1/(C_p - C_0)$ using the equation

$$1/\Delta F = 1/\Delta F_{max} + 1/(C_p - C_0) \tag{2}$$

Fluorescence titration was conducted at five different temperatures (20, 24, 26, 28, and 32 °C) to determine by means of van't Hoff equation the thermodynamic parameters ΔH, ΔS, and ΔG associated with the interaction:

$$\ln(K_a) = -(\Delta H/R)(1/T) + \Delta S/R \tag{3}$$

$$\ln(K_d) = (\Delta H/R)(1/T) - \Delta S/R \tag{4}$$

where R is the universal gas constant and T is the absolute temperature. The plot of $\ln(K_d)$ versus $1/T$ gives a straight line, with a slope of $\Delta H/R$ and an intercept of $-(\Delta S/R)$, from which van't Hoff enthalpy change and entropy change were calculated. ΔG was calculated from the relation

$$\Delta G = \Delta H - T\Delta S \tag{5}$$

The method of continuous variation (Job Plot) was employed to determine the stoichiometry of binding of ellipticine to H24.[10] The fluorescence of ellipticine at 520 nm was recorded at a constant temperature (24 °C) for pre-equilibrated reaction mixtures, in which number of moles of H24 and ellipticine in a fixed volume was varied, keeping the sum total number of moles and the reaction volume constant. The fluorescence of ellipticine under these conditions was plotted as a function of the input mole fraction of ellipticine. The point in the plot at which the two resulting straight lines meet corresponds to the mole fraction of ellipticine in the H24–ellipticine complex. The stoichiometry is obtained in terms of

$$\text{ellipticine: H24} = \chi_{ellipticine} : (1 - \chi_{ellipticine}) \tag{6}$$

where $\chi_{ellipticine}$ is the mole fraction of ellipticine calculated as the ratio of the molar concentration of ellipticine to the total molar concentration of H24 and ellipticine.

Isothermal Titration Calorimetry. ITC experiments were conducted in an iTC200 microcalorimeter (Microcal, Inc., Northampton, MA) at four temperatures between 24 and 36 °C. Samples were extensively degassed prior to titration. The titration of ellipticine against the G-quadruplex was performed by injecting H24 (700 μM in terms of base; 29.2 μM in terms of whole oligomer) into a solution with a fixed concentration of ellipticine (30 μM). A blank experiment in which H24 was injected into buffer containing the same volume percentage of DMSO (as ellipticine) was conducted to correct for dilution. The background was subtracted from the measured heats, and the corrected heats were plotted versus molar ratio. The corrected isotherms showed that only one type of binding event is taking place. The isotherms were analyzed using the built-in Microcal LLC ITC software. A "one set of sites" model yielded the best-fit curve for the obtained data points. The equilibrium association constant (K_a), enthalpy (ΔH), and entropy (ΔS) of association were obtained after each isotherm had been fit. The Gibbs energy was calculated using eq 5.

The change in heat capacity (ΔC_p) for the association of ellipticine with H24 was calculated from the slope of the plot of enthalpy change (ΔH) versus temperature. The slope of the plot of ΔH versus $T\Delta S$ gives the extent of enthalpy–entropy compensation for the interaction.

Circular Dichroism. CD spectra were recorded on a JASCO J715 spectropolarimeter (Jasco Corp., Tokyo, Japan) at 25 °C. The CD scans were recorded within the wavelength range of 220–400 nm with a scan speed of 200 nm/min and a step size of 0.2 nm. The time constant was 2 s, and the bandwidth was 1 nm. All measurements were taken in a 1 cm path length cuvette in a reaction volume of 2000 μL. A solution of H24 (3 μM) was titrated with increasing concentrations of ellipticine dissolved in DMSO. Each spectrum was an average of four runs. Each spectrum was recorded 5 min after each addition to ensure complete complex formation. Blank titration was conducted by adding an equal volume of DMSO without ellipticine to confirm that that DMSO does not cause any structural alteration of H24. Convex constraint analysis (CCA) was performed on the spectral set to extract the basis spectra and their associated coefficients.[11]

Differential Scanning Calorimetry. Excess heat capacity was measured as a function of temperature in a VP DSC microcalorimeter (Microcal, Inc.) to investigate the transition
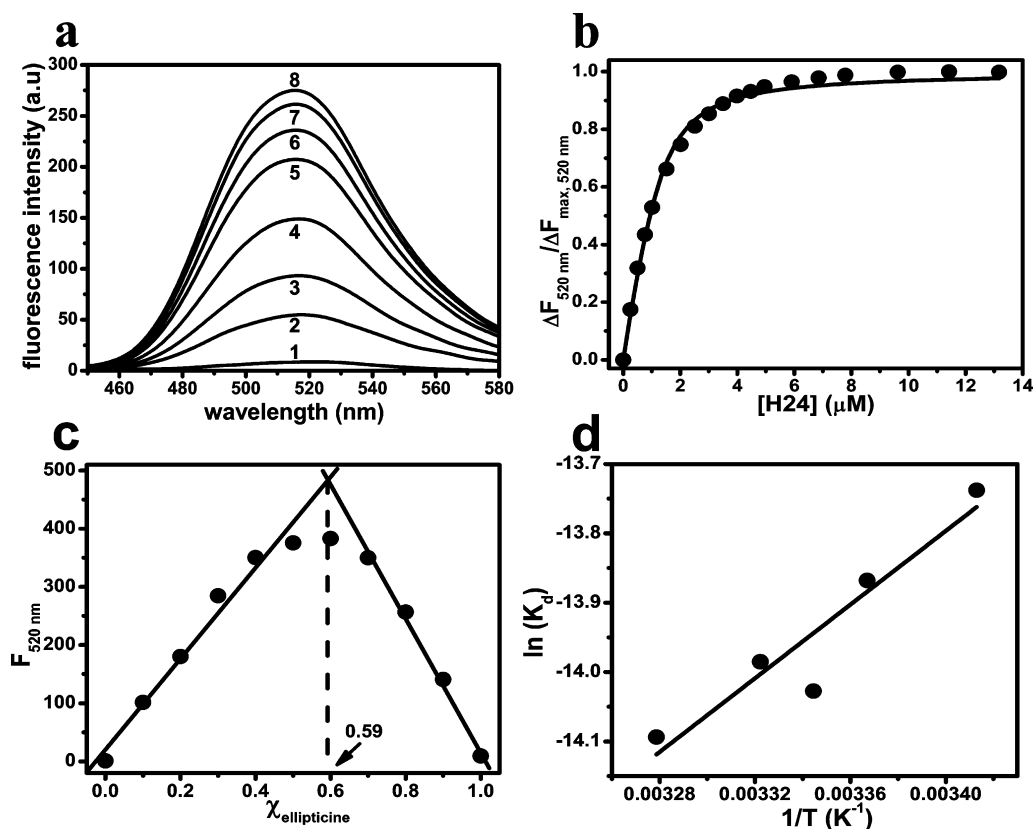
Figure 2. (a) Fluorescence spectra of 5 μM ellipticine in the presence of increasing concentrations of H24 (spectra 2−8 for 0.25, 0.50, 1.52, 2.51, 3.50, 5.91, and 13.17 μM H24, respectively) at 24 °C. (b) Curve fitting analysis of the binding isotherm obtained from fluorescence titration to evaluate the dissociation constant for the association of ellipticine with H24. The concentration at 50% value of $\Delta F_{520}/\Delta F_{max,520}$ provides the K_d (dissociation constant). (c) Job plot to determine the binding stoichiometry for association of ellipticine with H24. (d) van't Hoff plot to determine ΔH and ΔS for the ellipticine−H24 interaction. The solid line represents the best-fit linear curve through the obtained data points.

of quadruplex from the folded to the unfolded form in the absence and presence of ellipticine. The samples were scanned from 10 to 130 °C in the case of free H24 and from 20 to 130 °C in the case of H24 incubated with ellipticine and DMSO, at a scan speed of 60 °C/h at approximately 25 psi. Prior to the sample scan, the instrument was thermally stabilized by repeated buffer scans under similar conditions. H24 (80 μM) in buffer was scanned to obtain the melting profile of the unbound form. H24 (80 μM) was incubated for 1 h with 40 μM ellipticine and scanned to obtain the melting profile of the bound form. As a control, 80 μM H24 was incubated for 1 h with the same volume percent of DMSO and scanned to obtain the melting profile of H24 in DMSO. The thermograms obtained were analyzed using the built-in VPViewer software with Origin 7.0. The non-two-state (cursor initiation) model of curve fitting was used to fit the raw thermograms. Because $\Delta S° = \int[(\Delta C_p/T)/\Delta T]$, the area under the $\Delta C_p/T$ versus T plot yields $\Delta S°$.

Telomerase Repeat Amplification Protocol. The SYBR Green RQ-TRAP assay was conducted with cell extracts from MDAMB-231 breast cancer cells in 25 μL of reaction mixture with SYBR Green PCR Master Mix (US Biomax, Inc., Telomerase Detection Kit, MT3012). Quantitative real-time polymerase chain reaction (PCR) was used to study the *in vitro* effect of ellipticine on telomerase activity. Using ABI7500 Fast Real Time PCR, samples were incubated at 25 °C for 20 min and amplified via 40 PCR cycles for 30 s at 95 °C, 30 s at 60 °C, and 30 s at 72 °C (three-step PCR). PCR amplification

occurs in the second step of the PCR cycle. In this step, telomerase (from the cell extract) adds the telomeric repeat unit (TTAGGG) to the 3′ end of the TS primer (AATCC-GTCGAGCAGAGTT) present in the master mix. Fluorescence data were collected in the third PCR step. The threshold cycle values (C_t) were determined from the semilog amplification plot. C_t denotes the number of PCR cycles after which detectable fluorescence intensity is observed. The RQ-TRAP assay was conducted with 0, 2, and 4 μM ellipticine, keeping the reaction mixture volume fixed (25 μL). Each sample was analyzed in triplicate. The obtained C_t values at different ellipticine concentrations give an idea of the telomerase activity in the cell extract. From the observed C_t values, we can calculate the transformed fold change in telomerase activity with varying ellipticine concentrations. The transformed fold change in telomerase is calculated as follows[12]

$$\Delta C_t = C_{t,c} - C_{t,0} \qquad (7)$$

where $C_{t,c}$ is the average C_t value for a particular concentration (c micromolar) of ellipticine and $C_{t,0}$ is the average C_t value in the absence of ellipticine.

The fold change in telomerase activity due to the presence of ellipticine

$$X = 2 \exp(-\Delta C_t) \qquad (8)$$

$$\text{transformed fold change} = 1/X \qquad (9)$$

Table 1. Dissociation Constants and Thermodynamic Parameters for Binding of Ellipticine to H24 As Determined by Fluorescence Spectroscopy and Calorimetry in 10 mM Potassium Phosphate Buffer (pH 6.8) Containing 150 mM KCl at 24 °C

technique	K_d (μM)	N (ellipticine/H24)	ΔH (kcal mol^{-1})	$T\Delta S$ (kcal mol^{-1} K^{-1})	$\Delta G_{24\,°C}$ (kcal mol^{-1})
fluorescence (van't Hoff)	0.95	1.5	5.3 ± 1.1	13 ± 1.1	-8.2
isothermal titration calorimetry	1.5^a	1.5 ± 0.57	-1.4 ± 0.12	4.7	-6.1

^{a}For ITC, the dissociation constant obtained was divided by 24 to obtain the dissociation constant in terms of the whole oligomer.
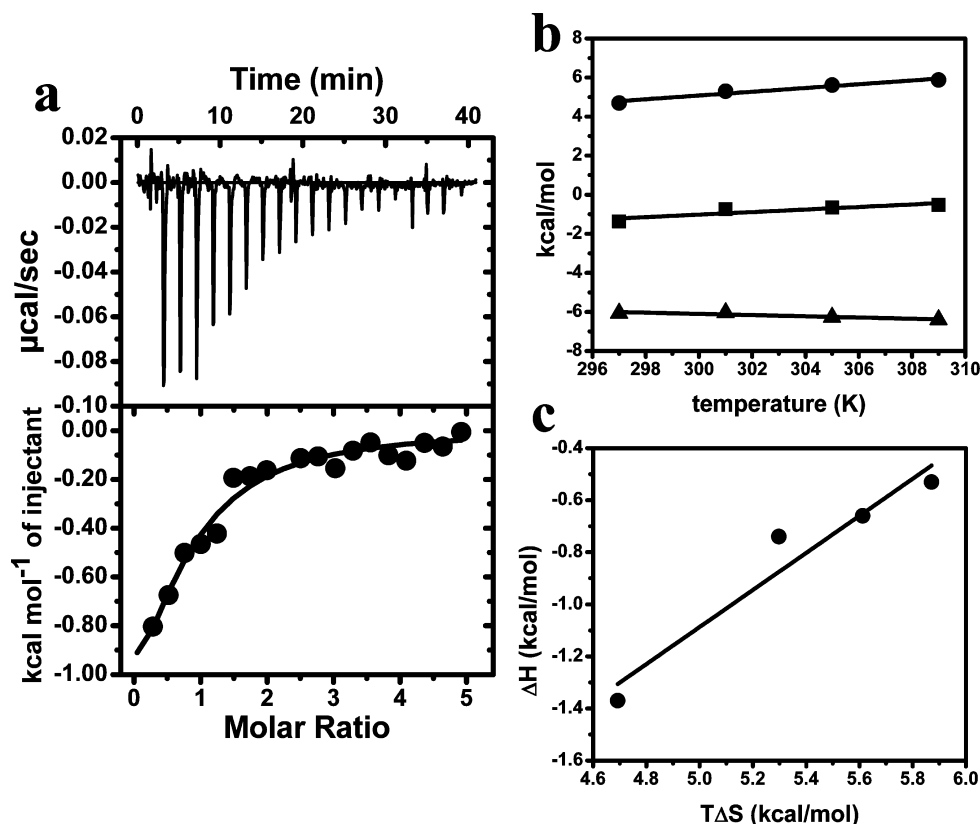

Figure 3. (a) ITC profiles for the titration of 700 μM H24 (in terms of base) into a 30 μM solution of ellipticine in 10 mM potassium phosphate buffer (pH 6.8) containing 150 mM KCl at 24 °C. The top panel shows the change in the differential power (DP) of the instrument. The bottom panel shows the binding isotherm resulting from integration of the peak area as a function of molar ratio. The solid line represents the calculated fit of the data. The dissociation constant obtained was divided by 24 to obtain the dissociation constant in terms of the whole oligomer. (b) Variation of thermodynamic parameters [ΔH (■), $T\Delta S$ (●), and ΔG (▲)] for the association of ellipticine with H24 as a function of temperature. A linear temperature dependence of enthalpy yields ΔC_p. (c) Enthalpy−entropy compensation plot for the interaction of ellipticine with H24.

■ RESULTS

Fluorescence Spectroscopy Studies. Results of fluorescence spectroscopy (Figure 2a) suggest association of H24 with ellipticine. This figure shows that the fluorescence intensity in the emission spectrum increases upon binding to H24. The change in the fluorescence intensity at 520 nm was plotted as a function of input H24 concentration and analyzed according to the technique described in Methods to determine the dissociation constant (Figure 2b).

The break point in the Job plot (Figure 2c) indicates the 2:3 binding stoichiometry (H24:ellipticine) of the complex.

Dissociation constants for the interaction of ellipticine with H24 were estimated at five different temperatures. The value of the dissociation constant of the interaction decreases with an increase in temperature. Analysis of the temperature dependence of the dissociation constant by the van't Hoff relationship (eq 4) yields the thermodynamic parameters (ΔH and ΔS) of the reaction (Figure 2d), which are listed in Table 1. Inspection

of thermodynamic data reveals positive ΔH and ΔS values for the association. The binding is entropically favorable.

Isothermal Titration Calorimetric Studies. ITC was conducted at four different temperatures to obtain the thermodynamic parameters for association of ellipticine with H24. The thermogram for binding of ellipticine to H24 at 24 °C is shown in Figure 3a. The association is characterized by small negative ΔH and large positive ΔS values at all temperatures as summarized in Table 2. The entropic contribution to the driving force of the reaction increases from ~77% at 24 °C to ~92% at 36 °C. The enthalpic contribution on the other hand decreases from ~23% at 24 °C to ~8% at 36 °C. This suggests that the interaction is an entropy-driven phenomenon at all temperatures. The slope of ΔH versus temperature yields the ΔC_p for the interaction, which is 65 ± 22 cal mol^{-1} K^{-1} (Figure 3b). The slope of 0.71 ± 0.13 (Figure 3c) for the plot of ΔH versus $T\Delta S$ gives an estimate of the extent of enthalpy−entropy compensation.

Circular Dichroism Studies. The CD spectrum of H24 is characterized by a positive band at 290 nm, a hump at 268 nm,

Table 2. Thermodynamic Parameters for the Association of H24 with Ellipticine As Determined by Isothermal Titration Calorimetry at Various Temperatures in 10 mM Potassium Phosphate Buffer (pH 6.8) Containing 150 mM KCl

temp (K)	ΔH (kcal mol^{-1})	$T\Delta S$ (kcal mol^{-1} K^{-1})	ΔG (kcal mol^{-1})	ΔC_p (cal mol^{-1} K^{-1})
297	-1.4 ± 0.12	4.7	-6.1	65 ± 22
301	-0.74 ± 0.09	5.3	-6.0	
305	-0.67 ± 0.06	5.6	-6.3	
309	-0.53 ± 0.06	5.9	-6.4	

and a negative band at 236 nm. In the presence of increasing concentrations of ellipticine, (i) the intensity of the peak at 290 nm increased, (ii) the intensity of the peak at 268 nm decreased, and (iii) an induced CD band originated at ~330 nm (Figure 4a,b). Because of the presence of DMSO in the system, the signal:noise ratio beyond 240 nm is very low. Thus, the spectral features beyond 240 nm were not considered. In the presence of DMSO, the basic spectral feature of H24 is unchanged with a positive band at 290 nm and a hump at 268 nm (Figure S1 of the Supporting Information), but because of interference from DMSO, the negative band at 236 nm cannot be distinguished. CCA analysis shows that the CD spectra of ellipticine-bound H24 can be best deconvoluted into two basis spectra (Figure 4c). One of these (component 1) is characteristic of the CD spectrum of unbound H24. The

other (component 2) represents the spectrum for ellipticine-bound H24. The variation of the associated coefficients of each basis spectrum was plotted as a function of ellipticine concentration (Figure 4d). It is characterized by a decrease in the percent population of component 1 and a concomitant increase in the percent population of component 2.

Differential Scanning Calorimetric Studies. To gain knowledge about the thermal stability of H24 in the absence and presence of ellipticine, DSC studies were performed. Repeated scans of the same sample for both the unbound and bound forms of H24 overlapped, indicating reversibility. The melting parameters are summarized in Table 3 and Table S1 of the Supporting Information.

H24 melting is characterized by two major thermal transitions, one at 49.92 °C and the other at 65.19 °C (Figure S2 of the Supporting Information). The observed melting transitions are consistent with earlier reports.[8] Because the buffer contains DMSO, oligomer melting was repeated in its presence (Figure 5a). There was no significant alteration in the profile or the melting temperature. It suggests that the observed effects of ellipticine as described below are not due to the artifact from the presence of DMSO. The limited solubility of ellipticine in buffer prevented us from scanning a sample consisting of only the H24–ellipticine complex. Upon forming a complex with ellipticine, H24 shows three melting transitions at 47.0, 66.1, and 76.3 °C (Figure 5b). While the first two melting transitions correspond to the melting of unbound H24,
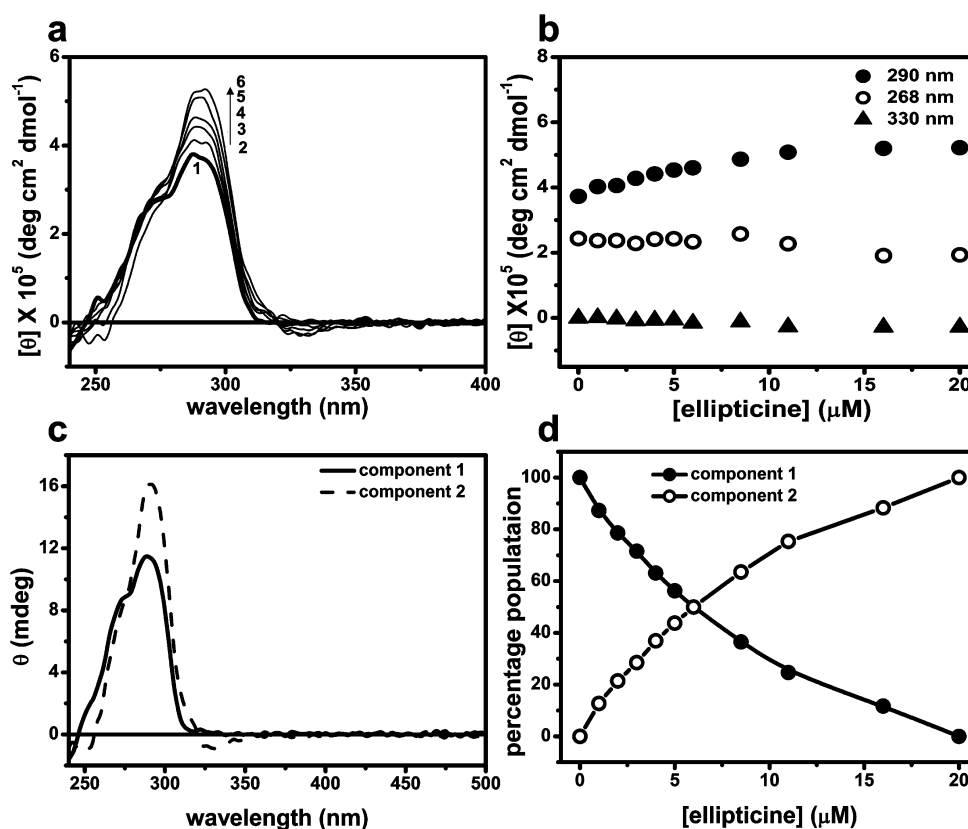

Figure 4. (a) Representative CD spectra resulting from the interaction of H24 (3 μM, spectrum 1) with an increasing ellipticine concentration (spectra 2–6 for 2, 4, 6, 11, and 20 μM ellipticine, respectively) in 10 mM potassium phosphate buffer (pH 6.8) containing 150 mM KCl at 25 °C. (b) Variation of molar ellipticity at three selected wavelengths [290 (●), 268 (○), and 330 nm (▲)] for H24–ellipticine interaction. (c) Basis spectra obtained from CCA analysis of CD spectra shown in panel a (component 1 is characteristic of the CD spectrum of unbound H24 represented by a solid line, and component 2 is characteristic of the CD spectrum of ellipticine-bound H24 represented by a dashed line). (d) Contribution of CCA components as a function of ellipticine concentration [component 1 (●) and component 2 (○)].

Table 3. Thermodynamic Parameters for the Intramolecular Quadruplex to Random Coil Transition, in the Absence and Presence of Ellipticine, for H24 in 10 mM Potassium Phosphate Buffer (pH 6.8) Containing 150 mM KCl As Determined by DSC

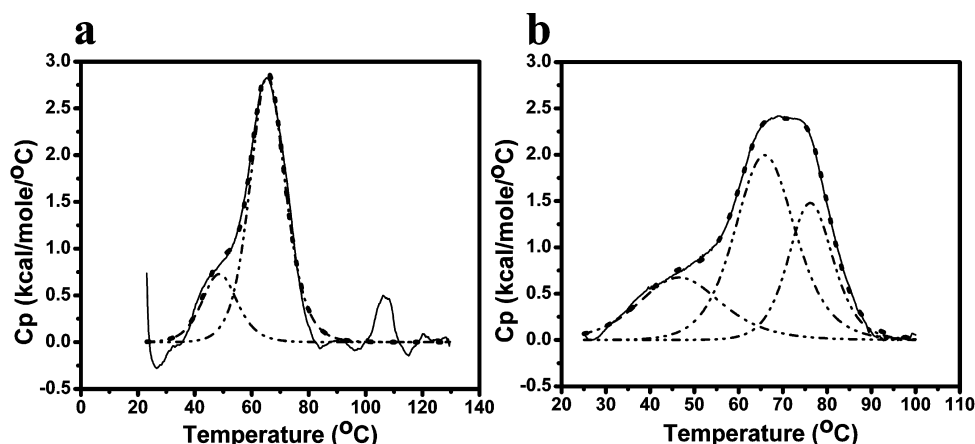| system	T_{m1} (°C)	$\Delta H_{cal,1}$ (kcal mol^{-1})	ΔS_1 (cal mol^{-1} K^{-1})	T_{m2} (°C)	$\Delta H_{cal,2}$ (kcal mol^{-1})	ΔS_1 (cal mol^{-1} K^{-1})	T_{m3} (°C)	$\Delta H_{cal,3}$ (kcal mol^{-1})	ΔS_1 (cal mol^{-1} K^{-1})
H24 in DMSO	48.8 ± 0.4	12.0 ± 0.8	37.2	65.7 ± 0.1	46.6 ± 0.8	138	–	–	–
H24 with ellipticine	47.0 ± 0.3	16.7 ± 0.6	51.0	66.1 ± 0.2	36.2 ± 1.6	106	76.3 ± 0.1	19.9 ± 1.2	56.9

Figure 5. Excess heat capacity profile for 80 μM H24 in the presence of (a) DMSO and (b) 40 μM ellipticine in 10 mM potassium phosphate buffer (pH 6.8) containing 150 mM KCl. The observed data (—) were deconvoluted (··—··) using the built-in "two-state" model for curve fitting software. The dashed curve denotes the overall fit of the data.

the third melting transition corresponds to the melting of ellipticine-bound H24. The higher melting temperature of bound H24 originates from ellipticine-induced stabilization of H24 structure.

Telomerase Repeat Amplification Protocol Studies. To question the relevance of association of ellipticine with telomere ends, we focused on testing whether ellipticine had any influence on telomerase activity. To assay telomerase activity, we used a very well established method, the telomeric repeat amplification protocol (TRAP) assay. This is a sensitive technique that allows telomerase detection in mammalian cell and tissue extracts even with very low telomerase activity levels. Quantification of telomerase activity (real-time monitoring of the TRAP assay product) in the presence of ellipticine gave a dose-dependent decrease in telomerase catalytic activity in cell lysates prepared from MDAMB-231 cells (Figure 6). This decrease was quantified by the number of threshold cycles

Figure 6. TRAP assay using RT-PCR to determine the concentration-dependent change in telomerase (extracted from MDAMB-231 cells). The experiments were run in triplicate with 0, 2, and 4 μM ellipticine.

needed to obtain detectable fluorescence intensity with an increasing amount of ellipticine during real-time TRAP. The telomerase activity decreases by 1.4-fold upon addition of 2 μM ellipticine and by 2.4-fold upon addition of 4 μM ellipticine to the cell extracts prior to the assay. These results showed that ellipticine negatively affects the typical six-nucleotide ladder of primer extension products characteristic of human telomerase in the TRAP assay.

■ DISCUSSION

Human telomeric DNA has emerged as a putative target for anticancer agents.[1] In the past few years, there has been a surge in studies involving small molecules that interact with telomeric DNA, thereby stabilizing them and inhibiting telomerase activity.[13−25] In this study, we report the interaction of ellipticine with the human telomeric DNA sequence, H24.

H24 adopts a (3+1) hybrid structure in K$^+$ ions with one double-chain reversal loop and two edgewise loops.[26−28] We have employed spectroscopic and calorimetric techniques to study the interaction between H24 and putative anticancer agent ellipticine. The major conclusions are as follows: (a) Ellipticine interacts with H24 with a very high affinity with a dissociation constant in the submicromolar range. (b) The H24:ellipticine binding stoichiometry is 2:3. (c) The association is entropy-driven as shown by both calorimetry and van't Hoff methods. (d) Association with ellipticine results in an enhancement of the melting temperature of H24 arising from the stability of the quadruplex structure. (e) No major structural change in H24 occurs when it binds to ellipticine as indicated from the analysis of ligand-induced CD spectra of the quadruplex. (f) Ellipticine effectively blocks telomerase activity in cell extracts from cancerous cell lines.
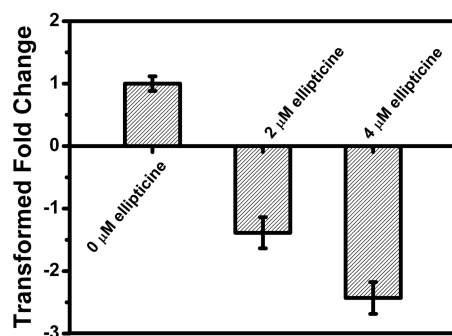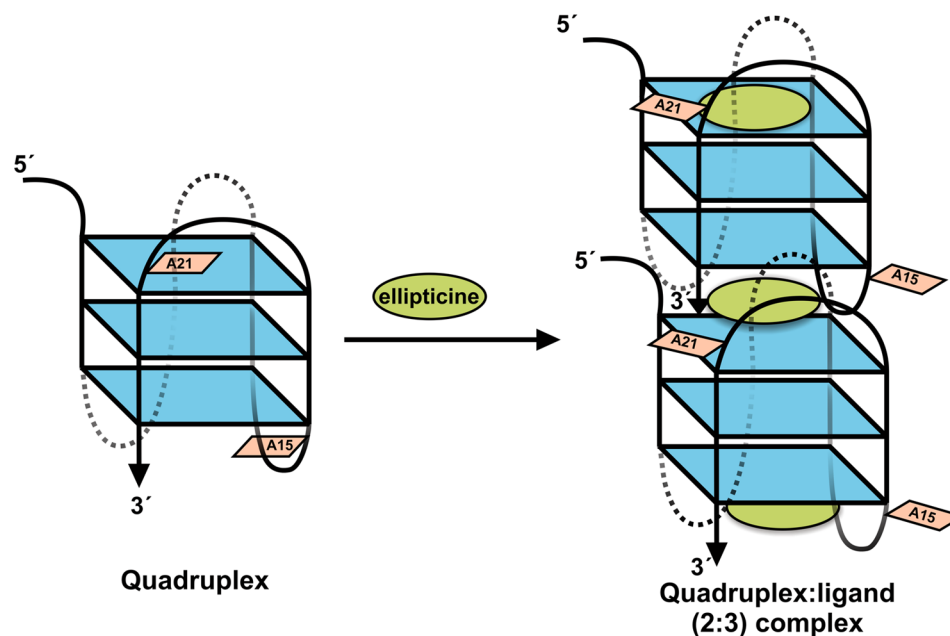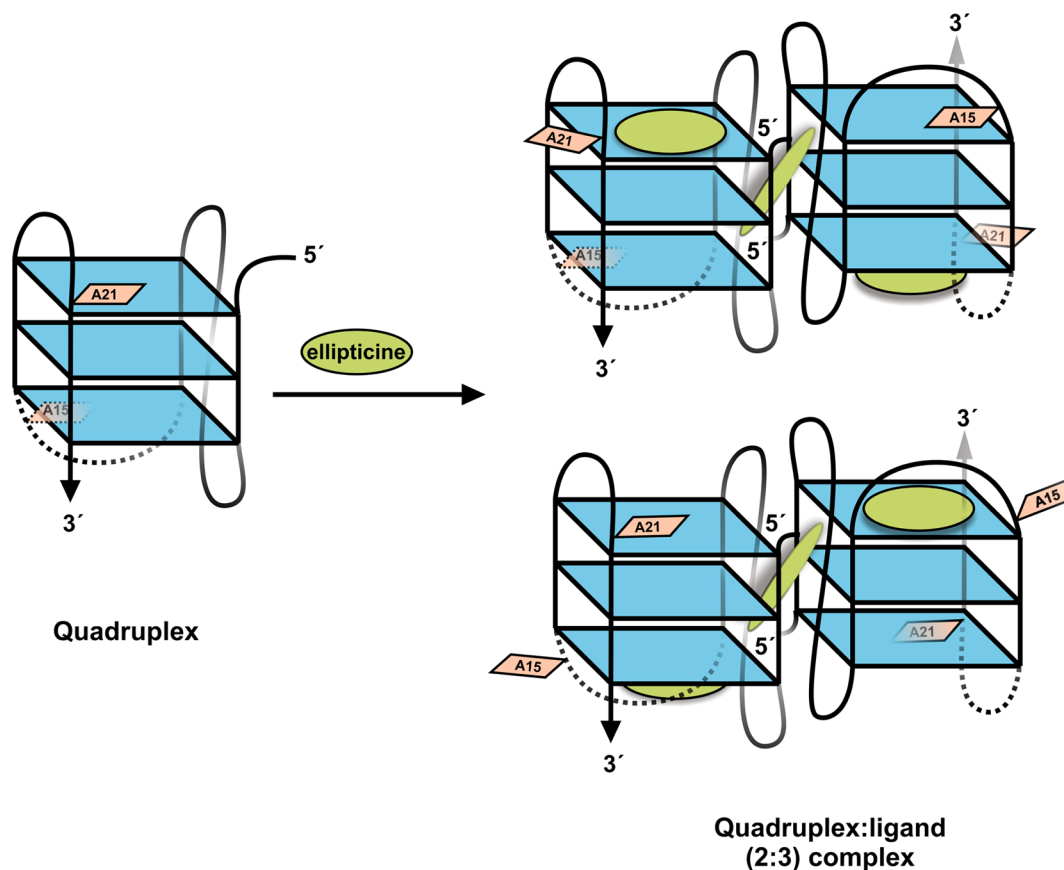
Scheme 1. Interaction between Ellipticine and (3+1) Hybrid Human Telomeric Quadruplex DNA (H24)[a]

[a]In the absence of any ligand, the two adenines in the edgewise loops (A15 and A21) are stacked on the terminal G-quartets. Two H24 moieties end stack on one another with an ellipticine molecule sandwiched between them. When the ligand binds, A15 and A21 become destacked.

Scheme 2. Interaction between Ellipticine and (3+1) Hybrid Human Telomeric Quadruplex DNA (H24)[a]

[a]In the absence of any ligand, the two adenines in the edgewise loops (A15 and A21) are stacked on the terminal G-quartets. Two H24 moieties are aligned side by side with an ellipticine molecule bound to the double-chain reversal loop. The adenine bases become destacked upon ligand binding.

Spectroscopic studies provide direct evidence of binding of ellipticine to H24. When ellipticine binds to H24, the fluorescence intensity and hence the quantum yield of ellipticine are found to increase. The increase in fluorescence

emission intensity may originate from one or more of the following factors: a change in the local environment such as viscosity or hydrophobicity of the ligand molecule, alteration in the conformation of the ligand molecule, and enhancement of the extent of excited state proton transfer.[29,30] Bound ellipticine is shielded from the surrounding solvent molecules, which in turn protect it from excited state deprotonation by the solvent molecules. The transfer of an excited state proton to an acceptor region present in the electronically deficient quartet planes of the quadruplex might also be a factor in the increase in the quantum yield of ellipticine upon association with the quadruplex molecule.

The binding stoichiometry indicates that three ellipticine molecules bind to two H24 molecules. This is possible only if one ellipticine molecule is sandwiched between two H24 molecules and one ellipticine molecule is bound to each of the two H24 moieties. It has been reported that planar aromatic compounds bind to the quadruplex via external end stacking (terminal capping) to the surface of the G-quartets on one or both ends of the quadruplex.[31−36] Binding of more than one ligand to a single quadruplex has been reported in the case of pentamethylated epigallocatechin derivatives,[37] porphyrins,[38,39] perylene derivatives,[40] phenanthroline derivatives,[41] plant alkaloids,[12,42−44] etc. Keeping in mind these reports and the observed binding stoichiometry, we propose that one ellipticine molecule end stacks on H24. Two such ellipticine−H24 complexes interact with each other and a third ellipticine molecule. We hypothesize that the third ellipticine molecule could either (a) intercalate between the complexes at the free end of the quartet (Scheme 1) or (b) bind to the double-chain reversal loop of both complexes (Scheme 2). If the third ellipticine molecule is intercalated between two H24 moieties, then we have two H24 molecules end stacking on one another. On the other hand, if the third ellipticine binds to the loop, we have two H24 moieties aligned side by side. The second hypothesis describing the binding geometry would result in a poor overlap between the loop bases and the planar ellipticine. Also, it is unlikely that a planar molecule like ellipticine can distinguish between two similar faces of the G-quartet and specifically bind to one of the faces of the quartet. In the alternate possibility of an end stacking geometry of an intercalated ellipticine between two H24 moieties, the overlap will occur to a greater extent with the quartet plane of the quadruplex. Both possibilities would lead to a 2:3 H24:ellipticine stoichiometry. The release of water molecules and counterions as a sequel to ligand binding would result in an increase in the entropy of the system.

The limited solubility of ellipticine prevented us from conducting a structural analysis of the H24−ellipticine complex using nuclear magnetic resonance, so we used CD spectroscopy to shed light on the ellipticine-induced structural alteration of the quadruplex. The CD spectra were deconvoluted using CCA analysis to obtain the composite spectra. CCA analysis suggests two composite spectra: one corresponding to the structure of the unbound oligomer and the other to the bound form. The presence of two basis spectra is also consistent with the analysis of the binding data. The CD spectral characteristics of the bound component show that bound H24 has a fold similar to that of the unbound form. The changes in the spectrum versus that of the free quadruplex can be ascribed to an alteration in the local environment of H24: destacking of the adenine bases in the loop region[35] and stacking of two ellipticine-bound H24

molecules with a third ellipticine molecule sandwiched between them.

While van't Hoff analysis suggests that the association of ellipticine with H24 is enthalpically unfavorable, calorimetric results suggest that the interaction, though entropically driven, has a small favorable enthalpy component in the free energy change. This enthalpic contribution to the free energy change decreases with an increase in temperature. The discrepancy in enthalpy values can be explained as follows.[45,46] ΔH_{cal} can be summed up as follows

$$\Delta H_{cal} = \Delta H_{association} + \Delta H_{concomitant}$$

where $\Delta H_{association}$ is the enthalpy change due to association of ellipticine with H24 and $\Delta H_{concomitant}$ is the enthalpy change due to other concomitant processes such as proton binding, ion binding, and conformational changes. On the other hand, ΔH_{VH}, obtained via the spectroscopic method, monitors only the enthalpy value arising from association process. Because spectroscopic techniques cannot monitor enthalpy changes from the spectroscopically silent processes, a discrepancy results.

Spectroscopic and calorimetric results prove that the interaction of ellipticine with H24 is an entropically driven phenomenon. There are two potential sources of the observed entropy-driven nature of the association. Release of water molecules and counterions as a sequel to binding of the ligand is one. The second source of favorable entropy originates from the destacking of the bases in the loop region of the quadruplex, which results in an increase in the configurational entropy of the oligomer. It has been shown earlier that the interaction of planar aromatic molecules with the (3+1) hybrid structure by terminal capping results in an increased mobility of the adenine residues in the edgewise loops (A15 and A21).[31,35] The binding-induced destacking of these bases leads to an increase in the configurational entropy of DNA. Association with ellipticine causes similar destacking of the adenine bases, which leads to a net increase in the entropy of the system.

Interaction of H24 with ellipticine gives rise to a small positive ΔC_p value. Heat capacity values are indicative of structural changes that occur as a sequel to binding. The relatively small magnitude of heat capacity change indicates that no major structural alteration of the quadruplex occurs as a sequel to binding. This is in accordance with our CD results that show that the binding, though characterized by a destacking of bases, does not cause any structural alteration of the mixed hybrid conformation of the quadruplex. A positive change in heat capacity is generally ascribed to the exposure of nonpolar groups to water.[47−50] Scrutiny of the structure of ellipticine tells us that the molecule is grossly nonpolar, with two polar regions at the two nitrogens. Interaction with H24 exposes the nonpolar region of ellipticine to water. This results in the positive ΔC_p value for the reaction. Positive changes in heat capacity may also arise from changes in soft internal vibration modes and temperature-dependent conformational changes and/or aggregation.[50] Aggregation of H24 as a sequel to ellipticine binding might be another reason for a positive ΔC_p for the system. The slope of ΔH versus $T\Delta S$ (enthalpy−entropy compensation plot) gives an estimate of the extent of enthalpy−entropy compensation for the reaction. A slope of unity indicates complete compensation of enthalpy by entropy. Deviation from unity indicates the predominance of one of the factors over the other. While for a slope of >1 the binding is primarily enthalpy-driven, for a slope of <1 the binding is

primarily entropy-driven.[51−53] A slope of 0.71 for ΔH versus $T\Delta S$ for H24−ellipticine interaction gives added support for the interaction being entropically driven.

The melting of H24[8] and H24 in the presence of DMSO is a three-step process involving an intermediate. The comparable melting profiles, temperatures, and ΔH_{cal} values of H24 in the absence and presence of DMSO indicate that DMSO does not affect the thermal stability and hence the macro structure of H24. H24 preincubated with ellipticine was scanned to determine the effect of the small molecule on the stability of H24. In presence of ellipticine, H24 shows three melting transitions (Table 3). The first two transitions correspond to the melting of free H24, while the third transition corresponds to the melting of H24 in a complex with ellipticine. The higher melting temperature of the H24−ellipticine complex suggests that end-stacked ellipticine stabilizes the H24 molecule as compared to free H24.

Results of the TRAP assay indicate that ellipticine binds to the quadruplex that forms at the end of the template primer and blocks the activity of telomerase, thereby inhibiting further elongation of the DNA template as the PCR cycle progresses. Considering telomerase activity to be 100% in the absence of ellipticine, it is seen that the telomerase activity is reduced by 28 and 59% upon addition of 2 and 4 μM ellipticine, respectively. It can thus be concluded that ellipticine effectively could impart its antineoplastic activity in a variety of cancer cell lines by downregulating the telomerase activity via stabilization of the telomeric DNA region.

Earlier reports have shown that ellipticine can inhibit the growth of MCF-7 breast adenocarcinoma cells in a concentration-dependent manner with an IC_{50} of 1.25 ± 0.13 μM.[54] It was proposed that the formation of ellipticine−DNA adducts may be the mechanism by which ellipticine imparts its anticancer activity in the cancer cell line. A recent report has also shown the presence of a GC-rich Sp1 binding region beginning at base pair −37 in relation to the TSS of the AHR promoter region in MCF-7 cancer cell lines.[55] The polymorphic $(GGGC)_n$ repeat is known to fold into quadruplex structures *in vitro* when $n \geq 2$. Thus, the possibility of other mechanisms involving association of ellipticine with quadruplex structures in the telomeric region and/or transcription start site (TSS) cannot be ruled out. We have shown in this study that ellipticine has a high affinity for quadruplex structures using H24 as a model. We can extrapolate our results to say that the G-rich region found in MCF-7 cell lines, with the potential to fold into quadruplex structure, may be a potential alternate target for ellipticine that has a high affinity for the higher-order DNA structures.

CONCLUSION

Ellipticine binds to telomeric DNA, H24, with high affinity. The interaction is entropically driven. This association stabilizes H24. CD signatures show that the overall fold of H24 is maintained upon ellipticine binding, though minor changes in the orientation of loop bases may occur to facilitate the binding of two ellipticine molecules and H24 stacking by one of the two molecules. The TRAP assay indicates that ellipticine blocks telomerase activity in extracts from cancer cell lines. Along with DNA intercalation and/or topoisomerase inhibition, ellipticine might also impart its antineoplastic activity via association with the DNA secondary structure, the G-quadruplex, which is a potential target for many anticancer agents.

ASSOCIATED CONTENT

Ⓢ Supporting Information

Thermodynamic parameters for melting, DSC melting profile of H24, and CD spectra of H24 in the presence of DMSO. This material is available free of charge via the Internet at http://pubs.acs.org.

AUTHOR INFORMATION

Corresponding Author

*Biophysics Division, Saha Institute of Nuclear Physics, Block-AF, Sector- I, Bidhan Nagar, Kolkata 700064, India. Phone: +91-33-2337-5345, ext. 3114. Fax: +91-33-2337-4637. E-mail: dipak.dasgupta@saha.ac.in.

Notes

The authors declare no competing financial interest.

ABBREVIATIONS

H24, human telomeric DNA sequence, 5′-d(TTAGGG)₄-3′; ITC, isothermal titration calorimetry; CD, circular dichroism; DSC, differential scanning calorimetry; TRAP, telomerase repeat amplification protocol.

REFERENCES

(1) Rezler, E. M., Bearss, D. J., and Hurley, L. H. (2002) Telomeres and telomerases as drug targets. *Curr. Opin. Pharmacol. 2*, 415−423.

(2) Dahse, R., Fiedler, W., and Ernst, G. (1997) Telomeres and telomerase: Biological and clinical importance. *Clin. Chem. 43*, 708−714.

(3) Auclair, C. (1987) Multimodal action of antitumor agents on DNA: The ellipticine series. *Arch. Biochem. Biophys. 259*, 1−14.

(4) Singh, M. P., Hill, G. C., Peoc'h, D., Rayner, B., Imbach, J. L., and Lown, J. W. (1994) High-field NMR and restrained molecular modeling studies on a DNA heteroduplex containing a modified apurinic abasic site in the form of covalently linked 9-aminoellipticine. *Biochemistry 33*, 10271−10285.

(5) Fosse, P., Rene, B., Charra, M., Paoletti, C., and Saucier, J. M. (1992) Stimulation of topoisomerase II-mediated DNA cleavage by ellipticine derivatives: Structure-activity relationship. *Mol. Pharmacol. 42*, 590−595.

(6) Froelich-Ammon, S. J., Patchan, M. W., Osheroff, N., and Thompson, R. B. (1995) Topoisomerase II binds to ellipticine in the absence or presence of DNA. Characterization of enzyme-drug interactions by fluorescence spectroscopy. *J. Biol. Chem. 270*, 14998−15004.

(7) Fung, S. Y., Duhamel, J., and Chen, P. (2006) Solvent effect on the photophysical properties of the anticancer agent ellipticine. *J. Phys. Chem. A 110*, 11446−11454.

(8) Antonacci, C., Chaires, J. B., and Sheardy, R. D. (2007) Biophysical characterization of the human telomeric (TTAGGG)$_4$ repeat in a potassium solution. *Biochemistry 46*, 4654−4660.

(9) Chakrabarti, S., Bhattacharyya, D., and Dasgupta, D. (2001) Structural basis of DNA recognition by anticancer antibiotics, chromomycin A3, and mithramycin: Roles of minor groove width and ligand flexibility. *Biopolymers 56*, 85−95.

(10) Huang, C. Y. (1982) Determination of binding stoichiometry by the continuous variation method: The job plot. *Methods Enzymol. 87*, 509−525.

(11) Perczel, A., Hollosi, M., Tusnady, G., and Fasman, G. D. (1991) Convex constraint analysis: A natural deconvolution of circular dichroism curves of proteins. *Protein Eng. 4*, 669−679.

(12) Ghosh, S., Pradhan, S. K., Kar, A., Chowdhury, S., and Dasgupta, D. (2013) Molecular basis of recognition of quadruplexes human telomere and c-myc promoter by the putative anticancer agent sanguinarine. *Biochim. Biophys. Acta 1830*, 4189−4201.

(13) Arthanari, H., and Bolton, P. H. (1999) Porphyrins can catalyze the interconversion of DNA quadruplex structural types. *Anti-Cancer Drug Des. 14*, 317−326.

(14) Franceschin, M., Rossetti, L., D'Ambrosio, A., Schirripa, S., Bianco, A., Ortaggi, G., Savino, M., Schultes, C., and Neidle, S. (2006) Natural and synthetic G-quadruplex interactive berberine derivatives. *Bioorg. Med. Chem. Lett. 16*, 1707−1711.

(15) Ghosh, S., Majumder, P., Pradhan, S. K., and Dasgupta, D. (2010) Mechanism of interaction of small transcription inhibitors with DNA in the context of chromatin and telomere. *Biochim. Biophys. Acta 1799*, 795−809.

(16) Gunaratnam, M., Greciano, O., Martins, C., Reszka, A. P., Schultes, C. M., Morjani, H., Riou, J. F., and Neidle, S. (2007) Mechanism of acridine-based telomerase inhibition and telomere shortening. *Biochem. Pharmacol. 74*, 679−689.

(17) Koeppel, F., Riou, J. F., Laoui, A., Mailliet, P., Arimondo, P. B., Labit, D., Petitgenet, O., Helene, C., and Mergny, J. L. (2001) Ethidium derivatives bind to G-quartets, inhibit telomerase and act as fluorescent probes for quadruplexes. *Nucleic Acids Res. 29*, 1087−1096.

(18) Rezler, E. M., Seenisamy, J., Bashyam, S., Kim, M. Y., White, E., Wilson, W. D., and Hurley, L. H. (2005) Telomestatin and diseleno sapphyrin bind selectively to two different forms of the human telomeric G-quadruplex structure. *J. Am. Chem. Soc. 127*, 9439−9447.

(19) Riou, J. F., Guittat, L., Mailliet, P., Laoui, A., Renou, E., Petitgenet, O., Megnin-Chanet, F., Helene, C., and Mergny, J. L. (2002) Cell senescence and telomere shortening induced by a new series of specific G-quadruplex DNA ligands. *Proc. Natl. Acad. Sci. U.S.A. 99*, 2672−2677.

(20) Seenisamy, J., Bashyam, S., Gokhale, V., Vankayalapati, H., Sun, D., Siddiqui-Jain, A., Streiner, N., Shin-Ya, K., White, E., Wilson, W. D., and Hurley, L. H. (2005) Design and synthesis of an expanded porphyrin that has selectivity for the c-MYC G-quadruplex structure. *J. Am. Chem. Soc. 127*, 2944−2959.

(21) Vy Thi Le, T., Han, S., Chae, J., and Park, H. J. (2012) G-quadruplex binding ligands: From naturally occurring to rationally designed molecules. *Curr. Pharm. Des. 18*, 1948−1972.

(22) Wei, C., Wang, J., and Zhang, M. (2010) Spectroscopic study on the binding of porphyrins to (G(4)T(4)G(4))4 parallel G-quadruplex. *Biophys. Chem. 148*, 51−55.

(23) Zhang, W. J., Ou, T. M., Lu, Y. J., Huang, Y. Y., Wu, W. B., Huang, Z. S., Zhou, J. L., Wong, K. Y., and Gu, L. Q. (2007) 9-Substituted berberine derivatives as G-quadruplex stabilizing ligands in telomeric DNA. *Bioorg. Med. Chem. 15*, 5493−5501.

(24) Zhou, J. L., Lu, Y. J., Ou, T. M., Zhou, J. M., Huang, Z. S., Zhu, X. F., Du, C. J., Bu, X. Z., Ma, L., Gu, L. Q., Li, Y. M., and Chan, A. S. (2005) Synthesis and evaluation of quindoline derivatives as G-quadruplex inducing and stabilizing ligands and potential inhibitors of telomerase. *J. Med. Chem. 48*, 7315−7321.

(25) Yang, D., and Okamoto, K. (2010) Structural insights into G-quadruplexes: Towards new anticancer drugs. *Future Med. Chem. 2*, 619−646.

(26) Luu, K. N., Phan, A. T., Kuryavyi, V., Lacroix, L., and Patel, D. J. (2006) Structure of the human telomere in K$^+$ solution: An intramolecular (3 + 1) G-quadruplex scaffold. *J. Am. Chem. Soc. 128*, 9963−9970.

(27) Phan, A. T., Kuryavyi, V., Luu, K. N., and Patel, D. J. (2007) Structure of two intramolecular G-quadruplexes formed by natural human telomere sequences in K$^+$ solution. *Nucleic Acids Res. 35*, 6517−6525.

(28) Phan, A. T., Luu, K. N., and Patel, D. J. (2006) Different loop arrangements of intramolecular human telomeric (3 + 1) G-quadruplexes in K$^+$ solution. *Nucleic Acids Res. 34*, 5715−5719.

(29) Aich, P., Sen, R., and Dasgupta, D. (1992) Role of magnesium ion in the interaction between chromomycin A3 and DNA: Binding of chromomycin A3-Mg^{2+} complexes with DNA. *Biochemistry 31*, 2988−2997.

(30) LePecq, J. B., and Paoletti, C. (1967) A fluorescent complex between ethidium bromide and nucleic acids. Physical-chemical characterization. *J. Mol. Biol. 27*, 87−106.

(31) Barbieri, C. M., Srinivasan, A. R., Rzuczek, S. G., Rice, J. E., LaVoie, E. J., and Pilch, D. S. (2007) Defining the mode, energetics and specificity with which a macrocyclic hexaoxazole binds to human telomeric G-quadruplex DNA. *Nucleic Acids Res. 35*, 3272−3286.

(32) Dhamodharan, V., Harikrishna, S., Jagadeeswaran, C., Halder, K., and Pradeepkumar, P. I. (2012) Selective G-quadruplex DNA stabilizing agents based on bisquinolinium and bispyridinium derivatives of 1,8-naphthyridine. *J. Org. Chem. 77*, 229−242.

(33) Haider, S. M., Neidle, S., and Parkinson, G. N. (2011) A structural analysis of G-quadruplex/ligand interactions. *Biochimie 93*, 1239−1251.

(34) Nicoludis, J. M., Barrett, S. P., Mergny, J. L., and Yatsunyk, L. A. (2012) Interaction of human telomeric DNA with N-methyl mesoporphyrin IX. *Nucleic Acids Res. 40*, 5432−5447.

(35) Pilch, D. S., Barbieri, C. M., Rzuczek, S. G., Lavoie, E. J., and Rice, J. E. (2008) Targeting human telomeric G-quadruplex DNA with oxazole-containing macrocyclic compounds. *Biochimie 90*, 1233−1249.

(36) Xue, L., Ranjan, N., and Arya, D. P. (2011) Synthesis and spectroscopic studies of the aminoglycoside (neomycin)−perylene conjugate binding to human telomeric DNA. *Biochemistry 50*, 2838−2849.

(37) Bai, L. P., Ho, H. M., Ma, D. L., Yang, H., Fu, W. C., and Jiang, Z. H. (2013) Aminoglycosylation can enhance the G-quadruplex binding activity of epigallocatechin. *PLoS One 8*, e53962.

(38) Wei, C., Jia, G., Yuan, J., Feng, Z., and Li, C. (2006) A spectroscopic study on the interactions of porphyrin with G-quadruplex DNAs. *Biochemistry 45*, 6681−6691.

(39) Nagesh, N., Sharma, V. K., Ganesh Kumar, A., and Lewis, E. A. (2010) Effect of ionic strength on porphyrin drugs interaction with quadruplex DNA formed by the promoter region of C-myc and Bcl2 oncogenes. *J. Nucleic Acids 2010*, 146418.

(40) Rao, L., Dworkin, J. D., Nell, W. E., and Bierbach, U. (2011) Interactions of a platinum-modified perylene derivative with the human telomeric G-quadruplex. *J. Phys. Chem. B 115*, 13701−13712.

(41) Wang, L., Wu, Y., Chen, T., and Wei, C. (2013) The interactions of phenanthroline compounds with DNAs: Preferential binding to telomeric quadruplex over duplex. *Int. J. Biol. Macromol. 52*, 1−8.

(42) Pradhan, S. K., Dasgupta, D., and Basu, G. (2011) Human telomere d[(TTAGGG)$_4$] undergoes a conformational transition to the Na$^+$-form upon binding with sanguinarine in presence of K$^+$. *Biochem. Biophys. Res. Commun. 404*, 139−142.

(43) Bazzicalupi, C., Ferraroni, M., Bilia, A. R., Scheggi, F., and Gratteri, P. (2012) The crystal structure of human telomeric DNA complexed with berberine: An interesting case of stacked ligand to G-tetrad ratio higher than 1:1. *Nucleic Acids Res. 41*, 632−638.

(44) Sassano, M. F., Schlesinger, A. P., and Jarstfer, M. B. (2012) Identification of G-Quadruplex Inducers Using a Simple, Inexpensive and Rapid High Throughput Assay, and Their Inhibition of Human Telomerase. *Open Med. Chem. J. 6*, 20−28.

(45) Faergeman, N. J., Sigurskjold, B. W., Kragelund, B. B., Andersen, K. V., and Knudsen, J. (1996) Thermodynamics of ligand binding to acyl-coenzyme A binding protein studied by titration calorimetry. *Biochemistry 35*, 14118−14126.

(46) Horn, J. R., Brandts, J. F., and Murphy, K. P. (2002) van't Hoff and calorimetric enthalpies II: Effects of linked equilibria. *Biochemistry 41*, 7501−7507.

(47) Baldwin, R. L. (1986) Temperature dependence of the hydrophobic interaction in protein folding. *Proc. Natl. Acad. Sci. U.S.A. 83*, 8069−8072.

(48) Makhatadze, G. I., and Privalov, P. L. (1990) Heat capacity of proteins. I. Partial molar heat capacity of individual amino acid residues in aqueous solution: Hydration effect. *J. Mol. Biol. 213*, 375−384.

(49) Spolar, R. S., Ha, J. H., and Record, M. T., Jr. (1989) Hydrophobic effect in protein folding and other noncovalent processes involving proteins. *Proc. Natl. Acad. Sci. U.S.A. 86*, 8382−8385.

(50) Sturtevant, J. M. (1977) Heat capacity and entropy changes in processes involving proteins. *Proc. Natl. Acad. Sci. U.S.A. 74*, 2236−2240.

(51) Sigurskjold, B. W., and Bundle, D. R. (1992) Thermodynamics of oligosaccharide binding to a monoclonal antibody specific for a *Salmonella* O-antigen point to hydrophobic interactions in the binding site. *J. Biol. Chem. 267*, 8371−8376.

(52) Brummell, D. A., Sharma, V. P., Anand, N. N., Bilous, D., Dubuc, G., Michniewicz, J., MacKenzie, C. R., Sadowska, J., Sigurskjold, B. W., Sinnott, B., Young, N. A., Bundle, D. R., and Narang, S. A. (1993) Probing the combining site of an anti-carbohydrate antibody by saturation-mutagenesis: Role of the heavy-chain CDR3 residues. *Biochemistry 32*, 1180−1187.

(53) Anbazhagan, V., Sankhala, R. S., Singh, B. P., and Swamy, M. J. (2011) Isothermal titration calorimetric studies on the interaction of the major bovine seminal plasma protein, PDC-109 with phospholipid membranes. *PLoS One 6*, e25993.

(54) Stiborova, M., Poljakova, J., Martinkova, E., Borek-Dohalska, L., Eckschlager, T., Kizek, R., and Frei, E. (2011) Ellipticine cytotoxicity to cancer cell lines: A comparative study. *Interdiscip. Toxicol. 4*, 98−105.

(55) Englert, N. A., Turesky, R. J., Han, W., Bessette, E. E., Spivack, S. D., Caggana, M., Spink, D. C., and Spink, B. C. (2012) Genetic and epigenetic regulation of AHR gene expression in MCF-7 breast cancer cells: Role of the proximal promoter GC-rich region. *Biochem. Pharmacol. 84*, 722−735.